Convective oscillations in a two-layer system under the combined action of buoyancy and thermocapillary effect

A.A. Nepomnyashchy [1], I.B. Simanovsky[1]

Summary

The convective oscillations in a two-layer system under the combined action of buoyancy and thermocapillary effect are studied in the framework of linear stability theory and by nonlinear simulations. It is shown that the influence of the thermocapillary effect supports the buoyancy-induced oscillations and can make them experimentally observable in the form of traveling waves. The thermocapillary oscillations appear in a subcritical way as standing waves. This instability mode is strongly suppressed by buoyancy, and it can be observed only under microgravity conditions.

Introduction

The stability problem for the mechanical equilibrium state in a fluid system with an interface is not self-adjoint (see, e.g. [1], [2]), thus an oscillatory instability is possible in both cases of buoyancy and thermocapillary convection. The buoyancy oscillatory instability was discovered by Gershuni and Zhukhovitsky [3]. However, the threshold Grashof number for the oscillatory instability was higher than that for the monotonic instability, that is why the oscillatory instability was not observable in experiments. The thermocapillary oscillatory instability was discovered by Sternling and Scriven [4] in the case of two semi-infinite layers and predicted for a real liquid system in [5].

In the present paper we investigate the oscillatory convection under the joint action of buoyancy and thermocapillary effect.

Formulation of the problem

We consider a system of two horizontal layers of immiscible viscous fluids with different physical properties. The system is bounded from above and from below by two isothermic rigid plates kept at constant different temperatures (the total temperature drop is θ). It is assumed that the interfacial tension σ decreases linearly with the increasing of the temperature: $\sigma = \sigma_0 - \alpha T$, where $\alpha > 0$.

The following notation is used: $\rho = \rho_1/\rho_2, \nu = \nu_1/\nu_2, \eta = \eta_1/\eta_2, \kappa = \kappa_1/\kappa_2, \chi = \chi_1/\chi_2, \beta = \beta_1/\beta_2, a = a_2/a_1$. Here ρ_m, ν_m, η_m, κ_m, χ_m, β_m and a_m are, respectively, density, kinematic and dynamic viscositiy, heat conductivity, thermal diffusivity, thermal expansion coefficient and the thickness of the m - th layer, where $m = 1$ ($m = 2$) corresponds to the top (bottom) layer. As the units of length, time, velocity, pressure and temperature we choose a_1, a_1^2/ν_1, ν_1/a_1, $\rho_1\nu_1^2/a_1^2$ and θ, respectively.

The nonlinear equations of convection in the framework of the Boussinesq approximation for both fluids have the following form ([1]):

[1]Department of Mathematics, Technion, 32000 Haifa, Israel

$$\frac{\partial \vec{v}_m}{\partial t} + (\vec{v}_m \cdot \nabla)\vec{v}_m = -e_m \nabla p_m + c_m \nabla^2 \vec{v}_m + b_m G T_m \vec{\gamma}, \frac{\partial T_m}{\partial t} + \vec{v}_m \cdot \nabla T_m = \frac{d_m}{P} \nabla^2 T_m, \nabla \cdot \vec{v}_m = 0.$$

Here $\vec{v}_m = (v_{mx}, v_{my}, v_{mz})$ is the velocity vector, T_m is the temperature and p_m is the pressure in the m - th fluid; $\vec{\gamma}$ is the unit vector directed upwards; $b_1 = c_1 = d_1 = e_1 = 1$; $c_2 = 1/\nu$, $d_2 = 1/\chi$, $e_2 = 1/\rho$; $G = g\beta_1 \theta a_1^3/\nu_1^2$ is the Grashof number and $P = \nu_1/\chi_1$ is the Prandtl number for the liquid in layer 1. The conditions on the isothermic rigid horizontal boundaries are:

$$z = 1: \quad \vec{v}_1 = 0; \quad T_1 = 0, \quad z = -a: \quad \vec{v}_2 = 0; \quad T_2 = s,$$

where $s = 1$ ($s = -1$) corresponds to heating from below (from above).

The deformation of the interface between two fluids can be usually neglected. In that case, the boundary conditions on the interface are:

$$z = 0: \quad \eta \frac{\partial v_{1x}}{\partial z} = \frac{\partial v_{2x}}{\partial z} + \frac{\eta M}{P} \frac{\partial T_1}{\partial x}, \quad \eta \frac{\partial v_{1y}}{\partial z} = \frac{\partial v_{2y}}{\partial z} + \frac{\eta M}{P} \frac{\partial T_2}{\partial x};$$

$$v_1 = v_2; T_1 = T_2; \kappa \frac{\partial T_1}{\partial z} = \frac{\partial T_2}{\partial z}.$$

Here $M = \alpha \theta a_1/\eta_1 \chi_1$ is the Marangoni number. For the comparison of the actions of thermocapillary effect and buoyancy, we use the inverse dynamic Bond number

$$K = \frac{M}{GP} = \frac{\alpha}{g\beta_1 \rho_1 a_1^2}.$$

The problem formulated above has a solution corresponding to the mechanical equilibrium. We investigate the linear stability of this solution. Also, we perform nonlinear simulations of two-dimensional flows by means of the finite-difference method (for details, see [1]).

Influence of thermocapillary effect on buoyancy-induced oscillations

We investigate the onset of the convection in the 47v2 silicone oil - water system with the following set of parameters: $\nu = 2.0$; $\eta = 1.7375$; $\kappa = 0.184$; $\chi = 0.778$; $\beta = 5.66$; $P = 25.7$; $a = 1.6$. This system was used in experiments on the convection in two-layer systems carried out in [6] that revealed convective oscillations.

The appearance of the "pure" buoyancy convection ($M = 0$) in each fluid layer is determined by the ratio of "local" Rayleigh numbers [1]

$$\frac{R_2}{R_1} = \frac{\kappa \nu \chi a^4}{\beta}.$$

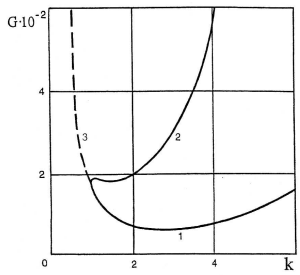

Figure 1: The neutral curves for $a = 1.6$; $R_2/R_1 = 0.328$; $K = 0$.

In our case $R_2/R_1 = 0.328 < 1$, therefore the lowest minimum corresponds to the onset of the monotonic Fig. 1, line 1). Line 2 corresponds to the linear instability boundary of the mechanical equilibrium with respect to the excitation of convection in a bottom layer. Merging of the monotonic neutral curves 1 and 2 leads to the appearance of a long-wave oscillatory neutral curve 3. However, no oscillatory nonlinear regimes can are observed.

Under the combined action of the thermocapillary effect and the buoyancy, the buoyancy volume forces and thermocapillary tangential stresses act in the opposite (similar) way with respect to the convection in the top (bottom) layer. Therefore, with the growth of K the instability boundary for the convection in the top (bottom) layer moves upwards (downwards). The oscillatory branch expands, and the minimum value of the Grashof number for the oscillatory instability curve decreases (Fig. 2). For $K_- < K < K_+$, $K_- \approx 0.328$, $K_+ \approx 0.411$, the minimum value of the Grashof number is achieved at the oscillatory branch of the neutral curve, therefore the oscillations become observable.

In our opinion, that can give the explanation of the waves found in experiments [6]. If we estimate $\alpha \sim 0.07$ dyn/cmK, which is a typical value for a silicone oil (the paper [6] does not contain measurements of α), we get $K = 0.33$, which is inside the interval where the observation of waves is predicted. The dimensional value of the critical temperature difference $\theta_c \approx 0.7$ K and the dimensional period of the linear oscillations $\tau_c \approx 670$ sec are in a reasonable coincidence with the experimental data ($\theta_{exp} \approx 0.63$ K, 7 $min < \tau_{exp} < 27$ min).

The results of the linear theory presented above are justified by the nonlinear simulations. It was found that the oscillatory instability generates traveling waves (see Fig. 3). Note that the same kind of the motion was observed in the experiments of Degen et al. [6].

Influence of buoyancy on thermocapillary oscillations

Later on, we deal with the system *n*-octane-methanol, which is an example of a physical system where the two-layer thermocapillary oscillations have been predicted by heating from above ($s = -1$) (see [5]). The ratios of the parameters are as follows: $\nu = 1.14$, $\eta = 1.02$, $\kappa = 0.698$, $\chi = 0.934$, $\beta = 0.963$, $Pr = 7.84$, $a = 1.6$. For these values of pa-

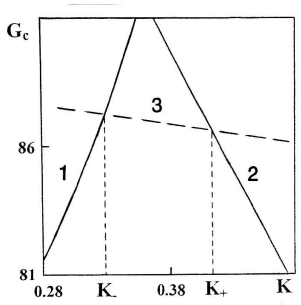

Figure 2: The critical Grashof number for the monotonic instabilities (lines 1, 2) and for the oscillatory instability (line 3).

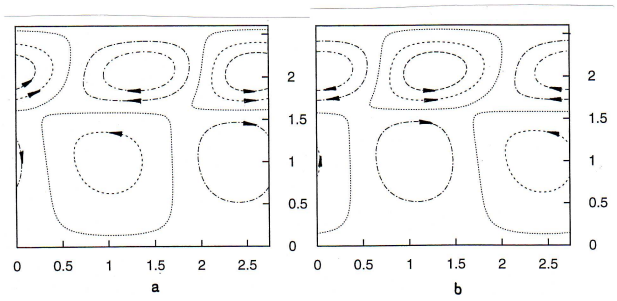

Figure 3: Snapshots of stream lines for the traveling wave at $a = 1.6$; $L = 2\pi/k = 2.74$; $G = 100$; $K = 0.4$. The wave moves from the right to the left.

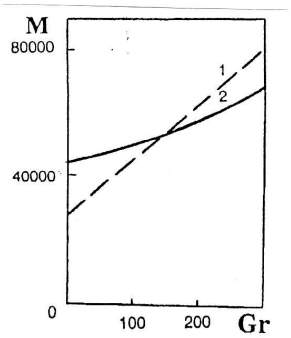

Figure 4: The dependences of the critical Marangoni number M on the Grashof number Gr for oscillatory (line 1) and monotonic (line 2) instabilities.

rameters, the threshold of the oscillatory instability is lower than that of the monotonic instability as $G = 0$ [5]. In the case of heating from above, the buoyancy effect prevents the onset of instability. Therefore, both monotonic and oscillatory instability thresholds increase with G. It is remarkable that the growth of the oscillatory instability threshold is faster than that of the monotonic instability (see Fig. 4). One has to take into account also the monotonic deformational instability mode with the threshold determined by the formula (2.75) in [1]:

$$M = sGa\delta\frac{2P(1+\eta a)(1+\kappa a)^2 a}{3\kappa(1+a)(1-\eta a^2)}, \text{ where } Ga = \frac{g a_1^3}{\nu_1^2}, \ \delta = \frac{\rho_2}{\rho_1} - 1.$$

Comparison of all the three competing instability modes shows that oscillatory instability cannot be observed in the case of normal gravity $g = g_0$. Under the microgravity, $g = g_0 \times 10^{-4}$, the oscillatory instability is predicted in the "window" $1.6 < a_1 < 2.4$ cm. For smaller thicknesses of the layers, the deformational instability will appear, while for larger thicknesses of the top layer one gets a monotonic non-deformational instability.

A weakly nonlinear bifurcation analysis at $G = 0$ [5] predicts a subcritical instability of the equilibrium state with respect to standing waves. This prediction was justified by our nonlinear simulations. In a cell with the aspect ratio $L = 3.6$, which contains exactly one period of the wave, we observed time-periodic standing waves. In a longer computational region, $L = 7.2$, the regular standing wave turned out to be unstable with respect to the spatiotemporal modluation. We observed the processes of creation and suppression of vortices that took place in an asymmetric, irregular way (see Fig. 5).

The inclusion of the non-zero Grashof number leads to regularization of the nonperiodic oscillations. With a further increase of the Grashof number the oscillations are completely suppressed.

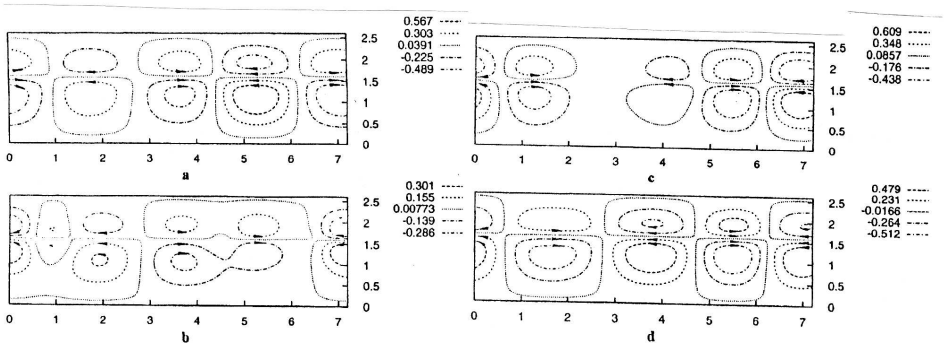

Figure 5: Stream lines (a)-(d) for the asymmetric nonperiodic motion; $L = 7.2$; $M = 3.07 \times 10^4$.

Reference

1. Simanovskii, I. B. and Nepomnyashchy, A. A. (1993): *Convective Instabilities in Systems with Interface, Gordon and Breach, London.*
2. Renardy, Y. Y. (1996): "Pattern formation for oscillatory bulk-mode competition in a two-layer Bénard problem", *Z. Angew. Math. Phys.*, Vol. 47, pp. 567-590.
3. Gershuni, G. Z. and Zhukhovitsky, E. M. (1982): "Monotonic and oscillatory instabilities of a two-layer system of immiscible liquids heated from below", *Sov. Phys. Dokl.*, Vol. 27, pp. 531-533.
4. Sternling, C. V. and Scriven, L. E. (1959): "Interfacial turbulence: Hydrodynamic instability and the Marangoni effect", *AIChE J.*, Vol. 5, pp. 514-523.
5. Colinet, P., Georis, Ph., Legros, J.-C., and Lebon, G. (1996): "Spatially quasiperiodic convection and temporal chaos in two-layer thermocapillary instabilities", *Phys. Rev. E*, Vol. 54, pp. 514-524.
6. Degen, M. M., Colovas, P. W., and Andereck, C. D. (1998): "Time-dependent patterns in the two-layer Rayleigh-Bénard system", *Phys. Rev. E*, Vol. 57, pp. 6647-6659.